Available online at www.sciencedirect.com
ScienceDirect
Scripta Materialia 57 (2007) 5–8
Scripta MATERIALIA
www.elsevier.com/locate/scriptamat

Shear bands at the fatigue crack tip of nanocrystalline nickel

Jijia Xie,* Xiaolei Wu and Youshi Hong

State Key Laboratory of Nonlinear Mechanics, Chinese Academy of Sciences, Beijing 100080, China

Received 7 January 2007; revised 3 March 2007; accepted 16 March 2007
Available online 16 April 2007

Fatigue crack growth rates in electrodeposited nanocrystalline Ni and its coarse counterpart were experimentally investigated in this paper. The shear bands, called the epsilon plastic zone, were observed on the surface of nanocrystalline Ni samples. The length of the shear bands is close to the estimated size of the plastic zone at the crack tip. Atomic force microscopy measurements indicate that the shear strain in the shear bands and the width of shear bands increase with related crack length.

Keywords: Nanocrystalline materials; Shear bands; Nickel; Fatigue; Crack tip

The mechanical properties of nanocrystalline (nc) and ultrafine-grained (ufg) materials have been widely studied in the past two decades, mostly due to the requirements for their use in applications. In particular, the propensities to fracture and fatigue are vital with respect to the application of nc materials. A number of experimental investigations about nc materials have been carried out (e.g. their production by equal channel angular pressing [1–10]). However, investigations into the fatigue properties of electrodeposited nc metal are limited.

Electrodeposited nc metal is often used as a model nc material in investigations due to its full density and quasi-equilibrium microstructure. For example, Hanlon et al. [11,12] investigated the fatigue properties of nc and ufg electrodeposited Ni. Their results indicated that, with grain refinement, the resistance to subcritical fatigue fracture decreased. Hanlon et al. also observed that the crack path tortuosity decreased with grain refinement. They proposed a crack deflection model to explain the relationship between this kind of tortuosity and the low resistance to subcritical fatigue crack propagation for nc Ni. The resistance to subcritical fatigue crack growth is related to the plasticity at the crack tip. However, the plastic zone at crack tips still requires further investigation.

With grain refinement, the deformation mechanism may vary. Some experimental investigations [13–16] indicate that grain boundary sliding is the prevailing mechanism of deformation for nc and ufg materials. Hugo et al. [17] and Kumar et al. [18] performed in situ tensile tests in a transmission electron microscope. Their observations reveal that dislocation-mediated plasticity plays a dominant role in the deformation of nc Ni. Farkas et al. [19] studied the crack propagation in nc Ni by using the molecular dynamics (MD) method. They observed that, at the crack tip, partial dislocation progressed sequentially from the grain boundary and resulted in the formation of full dislocations and twinning in the grain. Wu et al. [20,21] confirmed the existence of partial dislocation and twinning in nc materials, but their results were not obtained from the crack tip. Because of the limitation of the MD method and the lack of experimental evidence, the mechanism of deformation and crack propagation of nc materials is still not very clear. An alternative deformation mechanism may change the energy dissipation mode at the fatigue crack tip. Therefore, it is necessary to observe the plastic zone at the crack tip more accurately.

The objective of this paper is to investigate the differences between the subcritical crack growth mechanisms in nc electrodeposited Ni and its coarse counterpart. Optical microscopy (OM) and atomic force microscopy (AFM) were used to characterize the plastic zone at the crack tip. Scanning electron microscopy (SEM) was used to examine the fracture surface of the fatigue samples after break.

Electrodeposited nc Ni sheets, 120 μm thick, were purchased from Integran Technologies Inc. (Toronto, Canada). The average grain size was measured to be

* Corresponding author. E-mail: xiejj@lnm.imech.ac.cn

1359-6462/$ - see front matter
doi:10.1016/j.scriptamat.2007.03.027

26 nm by image analysis of the TEM pictures. Coarse-grained (cg) Ni sheets, 180 μm thick, were used in this paper for comparison with the nc Ni, which was annealed at 450 °C for 5 h to give an average grain size of 42 μm.

Fatigue crack growth experiments for the nc and cg Ni foils were conducted using edge-notched samples, 20 mm long and 5 mm wide. An edge notch of about 0.3 mm length was electro-discharge machined.

Fatigue crack growth tests were performed on an MTS 810 servohydraulic material test system. Fatigue cracks were initiated in cyclic tension loading at a stress ratio of 0.1 and a cycle frequency of 25 Hz at room temperature. The waveform is sinusoidal. Fatigue crack growth rates were measured using remote OM. Images of fatigue crack with different lengths were taken at different cycles of loading. The fracture surfaces were examined with an FEI Sirion400nc scanning electron microscope. OM was used to observe the crack growth path of samples after fatigue test. AFM was used to measure the contour of the sample surface at the fatigue crack tip.

Based on image analysis data, the variation of crack length vs. the number of fatigue cycles for the nc and cg Ni can be obtained. The variation of fatigue crack growth rate da/dN with ΔK_I in the Paris regime is plotted in Figure 1. It is seen that the crack growth rate of nc Ni is higher than that of cg Ni at the same ΔK_I.

Figure 2 presents two examples of fatigue crack path from two sample surfaces, showing that the crack path of nc Ni is very straight, whereas the crack path of cg Ni is zigzagged.

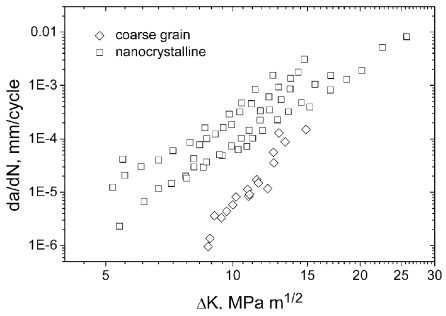

Figure 1. Variation of fatigue crack growth rate da/dN with ΔK_I.

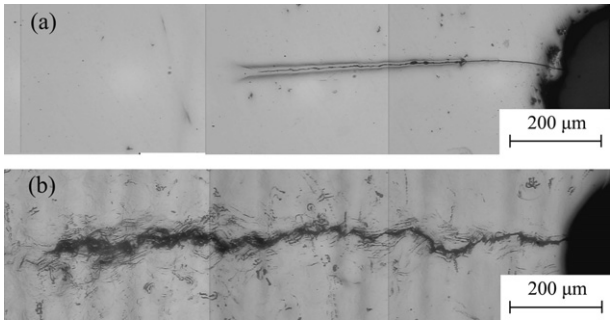

Figure 2. Fatigue crack propagation path of (a) an nc Ni sample and (b) a cg Ni sample.

Figure 3a is the image of a crack tip from an nc Ni sample. At the crack tip, shear bands formed periodically. The shear band pairs create a fishbone structure along the crack path. As shown in Figure 3b, the shear band on the surface matches one to one with the fatigue striations on the fracture surface.

In Figure 4, the crack propagation rate was compared with the spacing between two neighboring shear bands, which was measured on an optical image of the crack. The crack propagation length at each cycle and the space between shear bands are seen to be almost the same.

Figure 5 shows the shear band length measured on the crack image. The estimated size of the plastic zone under plane strain at the crack tip is also shown, as the solid curve, in this figure. Their values are very similar. With the increase in crack length, the stress condition changes from plane strain to plane stress. For this

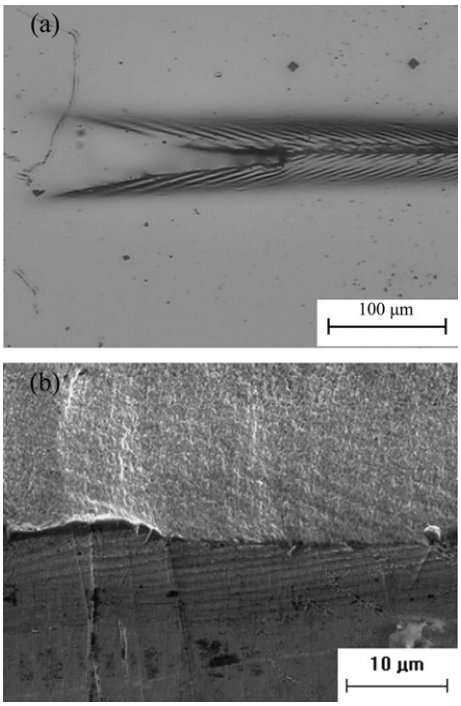

Figure 3. (a) An OM image showing a fatigue crack of an nc Ni sample with shear bands pairs. (b) A tilt SEM image showing shear bands and fatigue striations on the fracture surface.

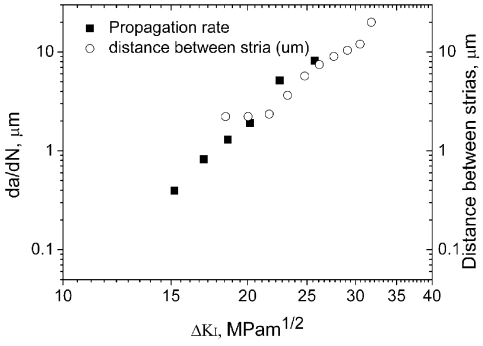

Figure 4. Crack growth rate and shear band spacing versus stress intensity factor at the crack tip.

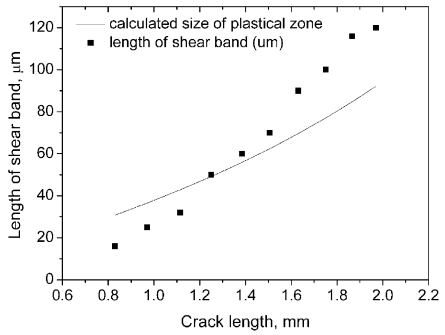

Figure 5. Shear band length versus crack length. The solid curve indicates the estimated plastic zone size under plane strain at the crack tip.

reason, when the crack length increases, the shear band length becomes larger than the size of the plastic zone under plane strain.

Figure 6 shows an AFM image of shear bands at the crack tip. The step height H, the project width L of shear bands along the normal direction of the fracture surface on the sample surface and the angle α between the shear bands on the sample surface and the crack can be measured. The equations describing the geometrical relationships between these values are as follows:

$$\begin{aligned} &\frac{w\gamma}{\sqrt{2}}\sqrt{1-(\tan(\alpha))^2} = H \\ &\sqrt{2}w + \frac{w\gamma}{\sqrt{2}}\left(1-(\tan(\alpha))^2\right) = L, \end{aligned} \tag{1}$$

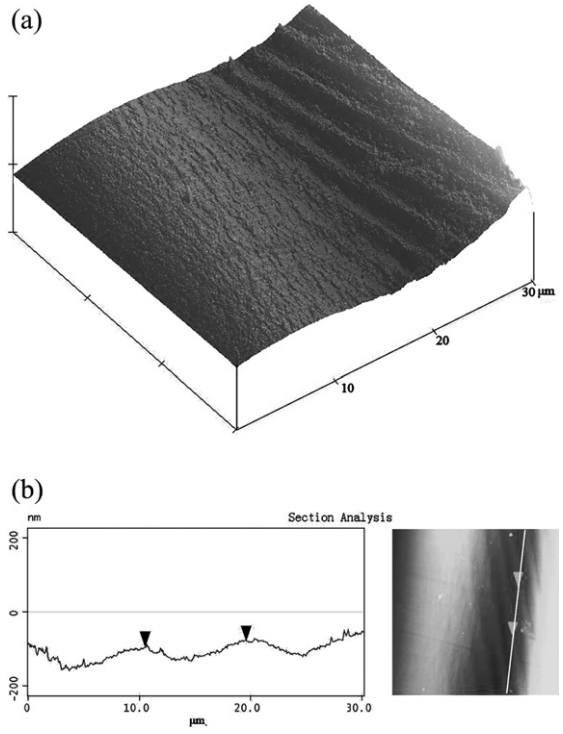

Figure 6. AFM image of shear bands along the fatigue crack of nc Ni. Scan area: 30 μm × 30 μm. (a) Three-dimensional map; (b) section analysis map.

Table 1. Shear band width and shear strain in shear bands at different crack lengths

Crack length (mm)	Step height H (μm)	Angle between shear bands and crack α (degrees)	Shear bands width w (μm)	Shear strain in shear bands γ
1.9	0.1438	19	0.858	0.253
1.69	0.0734	18.2	0.531	0.207
1.32	0.0483	21.9	0.429	0.174
1.055	0.0362	31.7	0.390	0.167

where w is the width of shear bands and γ is the shear strain in the shear bands. The results of these equations for different crack lengths are shown in Table 1. It seems that the width of the shear bands increases with the crack length. The shear strain in the shear bands also increases with the crack length.

According to Irwin, the size of plastic zone at the crack tip can be estimated by Eq. (2).

$$c = \frac{1}{3\pi}\left(\frac{K_1}{\sigma_y}\right)^2, \tag{2}$$

where σ_y is the yield stress and K_I is the stress intensity factor. In this investigation, the yield stress of nc Ni is 1200 MPa and that of cg Ni is 568 MPa. For a sample under the load range shown in Figure 1, the size of the plastic zone, normalized by the grain size, ranges from 89.5 to 778 for nc Ni and from 1.30 to 4.55 for cg Ni. This means that the size of the plastic zone is much greater than the grain size for nc Ni, but is approximately equal to the grain size for cg Ni. Therefore, the propagation path of the fatigue crack changed with the orientation of the grains at the front of the crack tip for cg Ni, but not for nc Ni.

In the work of Hanlon et al. [12], a crack deflection model was used to rationalize the decrease in fatigue crack growth rate in coarser grained samples. However, this is not sufficient. Because of the deformation at the crack tip of nc Ni is of shear band mode, the real volume of the plastic zone of nc Ni is much less than that of cg Ni. So, the difference in the values of plasticity at the crack tip between nc Ni and cg Ni can be very large. A higher degree of plasticity will lead to higher crack growth resistance.

Shear band pairs observed in the present investigation were called ε plastic zones in Takemori's work on fatigue fracture of a polycarbonate [22,23], in which the ε plastic zones were observed at the stage of localized discontinuous crack growth. Takemori found that crack propagation to be discontinuous. Shear band pairs grow from the crack tip first. After several load cycles, the crack jumped along the direction of the crack. In this investigation, as shown in Figure 4, the crack growth rate was equal to the spacing between the shear bands. This indicates that, in contrast to the case of the polycarbonate, the crack jump occurred at each cycle of load for nc Ni.

With the aid of AFM, the shear strain in shear bands was estimated to be about 0.20. It is about one order of magnitude larger than that measured in tensile testing.

Obviously, this is related to the stress condition. The length of shear bands at the crack tip is limited by the size of plastic zone, so the shear bands at crack tip will not propagate to break the sample.

Several experiments [4,10,24] on nc or ufg materials have reported shear bands occurring after loading. Considering shear band localization as the basic deformation mode for glass metals, the shear band mode might be an intrinsic phenomenon of materials with fine microstructure. This instability was attributed to the diminishing strain hardening capacity and low strain rate sensitivity of the flow stress in these nc and ufg materials. The observation of TEM pictures from Wei et al. [24] indicated that the deformation mechanism in shear bands is dislocation-mediated. However, the average grain size of their samples was 268 nm. The shear localization mechanism in materials with a grain size less than 100 nm is still under investigation. Although there is difficulty in the preparation of TEM samples, it is necessary to further observe the microstructure in the shear bands directly via TEM.

In summary, the measurements of fatigue crack growth rates of nc Ni and cg Ni indicate that the grain refinement reduces the resistance to subcritical fatigue fracture. The ε shear bands prevail on the nc Ni specimens along the fatigue crack. The length of shear bands is close to the estimated size of the plastic zone at the crack tip. The shear strain in the shear bands increases with the crack length.

This work was supported by National Natural Science Foundation of China (10472117, 50471086, 50571110), National Key Basic Research and Development Program of China (2004CB619305).

[1] M.A. Meyers, A. Mishra, D.J. Benson, Prog. Mater. Sci. 51 (2006) 427–556.
[2] R.Z. Valiev, R.K. Islamgaliev, I.V. Alexandrov, Prog. Mater. Sci. 45 (2) (2000) 103–189.
[3] S.R. Agnew, J.R. Weertman, Mater. Sci. Eng. A 244 (1998) 145–153.
[4] V. Patlan, A. Vinogradov, K. Higashi, K. Kitagawa, Mater. Sci. Eng. A 300 (2001) 171–182.
[5] A. Vinogradov, S. Hashimoto, Mater. Trans. 42 (1) (2001) 74–84.
[6] A.Y. Vinogradov, V.V. Stolyarov, S. Hashimoto, R.Z. Valiev, Mater. Sci. Eng. A 318 (2001) 163–173.
[7] H. Mughrabi, H.W. Hoppel, M. Kautz, Scripta Mater. 51 (2004) 807–812.
[8] M.D. Chapetti, H. Miyata, T. Tagawa, T. Miyata, M. Fujioka, Mater. Sci. Eng. A 381 (2004) 331–336.
[9] C.S. Chung, J.K. Kim, H.K. Kim, W.J. Kim, Mater. Sci. Eng. A 337 (2002) 39–44.
[10] S.D. Wu, Z.G. Wang, C.B. Jiang, G.Y. Li, I.V. Alexandrov, R.Z. Valiev, Mater. Sci. Eng. A 387–389 (2004) 560–564.
[11] T. Hanlon, Y.-N. Kwon, S. Suresh, Scripta Mater. 49 (2003) 675–680.
[12] T. Hanlon, E.D. Tabachnikova, S. Suresh, Int. J. Fatigue 27 (2005) 1147–1158.
[13] N. Yagi, A. Rikukawa, H. Mizubayashi, H. Tanimoto, Mater. Sci. Eng. A 442 (1–2) (2006) 323–327.
[14] N.Q. Chinh, P. Szommer, Z. Horita, T.G. Langdon, Adv. Mater. 18 (2006) 34–39.
[15] N. Wang, Z. Wang, K.T. Aust, U. Erb, Mater. Sci. Eng. A 237 (2) (1997) 150–158.
[16] W.M. Yin, S.H. Whang, R.A. Mirshams, Acta Mater. 53 (2005) 383–392.
[17] R.C. Hugo, H. Kung, J.R. Weertman, R. Mitra, J.A. Knapp, D.M. Follstaedt, Acta Mater. 51 (2003) 1937–1943.
[18] K.S. Kumar, S. Suresh, M.F. Chisholm, J.A. Horton, P. Wang, Acta Mater. 51 (2003) 387–405.
[19] D. Farkas, S. Van Petegem, P.M. Derlet, H. Van Swygenhoven, Acta Mater. 53 (2005) 3115–3123.
[20] Xiao-Lei Wu, En Ma, Appl. Phys. Lett. 88 (2006) 061905.
[21] X. Wu, Y.T. Zhu, M.W. Chen, E. Ma, Scripta Mater. 54 (2006) 1685–1690.
[22] Michael T. Takemori, Ann. Rev. Mater. Sci. 14 (1984) 171–204.
[23] Michael T. Takemori, Poly. Eng. Sci. 22 (15) (1982) 937–945.
[24] Q. Wei, D. Jia, K.T. Ramesh, E. Ma, Appl. Phys. Lett. 81 (7) (2002) 1240–1242.